Geosci. Model Dev. Discuss., 6, 6459–6492, 2013
www.geosci-model-dev-discuss.net/6/6459/2013/
doi:10.5194/gmdd-6-6459-2013

Geoscientific Model Development Discussions
Open Access

An improved non-iterative surface layer flux scheme for atmospheric stable stratification condition

Y. Li[1,2], Z. Gao[1,2], D. Li[3], L. Wang[2], and H. Wang[1]

[1]College of Applied Meteorology, Nanjing University of Information Science and Technology, Nanjing, Jiangsu, China
[2]State Key Laboratory of Atmospheric Boundary Layer Physics and Atmospheric Chemistry, Institute of Atmospheric Physics, Chinese Academy of Sciences, Beijing, China
[3]Department of Civil and Environmental Engineering, Princeton University, Princeton, NJ 08540, USA

Received: 29 October 2013 – Accepted: 25 November 2013 – Published: 5 December 2013

Correspondence to: Z. Gao (zgao@mail.iap.ac.cn)

Published by Copernicus Publications on behalf of the European Geosciences Union.

Abstract

Parameterization of turbulent fluxes under stably stratified conditions has always been a challenge. Current surface fluxes calculation schemes either need iterations or suffer low accuracy. In this paper, a non-iteration scheme is proposed to approach the classic iterative computation results using multiple regressions. It can be applied to the full range of roughness status $10 \le z/z_0 \le 10^5$ and $-0.5 \le \log(z_0/z_{0h}) \le 30$ under stable conditions $0 < Ri_B \le 2.5$. The maximum (average) relative errors for the turbulent transfer coefficients for momentum and sensible heat are 12 % (1 %) and 9 % (1 %), respectively.

1 Introduction

In weather or climate models, earth surface is the boundary that needs to be resolved physically (Chen and Dudhia, 2001). The condition of atmosphere aloft (e.g., wind, temperature and humidity) is highly dependent on the momentum, sensible heat and latent heat fluxes at surface. Currently, the exchanges of momentum and heat between the earth surface and the atmosphere are usually calculated with various schemes based on Monin–Obukhov similarity theory (hereinafter MOST, Monin and Obukhov, 1954) in models. These schemes (e.g., Paulson, 1970; Businger, 1971; Dyer, 1974; Holtslag and De Bruin, 1988; Beljaars and Holtslag, 1991; Janjić 1994; Launiainen, 1995; Hogstrom, 1996) are similar to each other but the differences among them exist due to different observational data and/or mathematical solutions that were used in retrieving the schemes. One commonly used scheme is Businger–Dyer (B-D) equation (Businger, 1966; Dyer, 1967). However, the BD equation suppresses fluxes under stable condition too quickly and is not applicable when the Richardson number exceeds a critical value (Louis, 1979). Holtslag and De Bruin (1988) and Beljaars and Holtslag (1991) proposed alternative schemes which can be used under very stable conditions. Cheng and Brutsaert (2005, CB05 hereinafter) further provided a new scheme and it is confirmed to perform better by later research (Guo and Zhang, 2007; Jimenez et al., 2012).

A critical issue regarding the fluxes calculation with MOST is the numerical iteration. Under unstable condition, the iteration normally converges within 5 steps (Fairall et al., 1996). In the WRF model (Skamarock et al., 2008), the flux variables from the previous time step are used to calculate the fluxes at current time step and such an approach can yield reasonable result (Jimenez et al., 2012). On the other hand, under stable condition, the flux calculation takes many more steps to converge and hence is time consuming. To avoid the iteration process, a series of non-iterative schemes are proposed (e.g., Loius, 1979; Garratt, 1992; Launiainen, 1995; Song, 1998; De Bruinet al., 2000; Yang et al., 2001; Li et al., 2010), but they all fail to cover the full range of $-0.5 \le kB^{-1} \le 30$, $10 \le z/z_0 \le 10^5$ and $-5.0 \le Ri_B \le 2.5$, which is pointed out by Wouters et al. (2012, WRL12 hereinafter). Here $kB^{-1} = \ln(z_0/z_{0h})$. z is the reference height; and z_0 and z_{0h} are the aerodynamic and thermal roughness lengths, respectively. Ri_B is the bulk Richardson number. To calculate fluxes under all conditions, and also to include the roughness sublayer effect, WRL12 proposed an updated scheme. However, for a given Ri_B, WRL12 uses only one equation to cover the whole large range of z/z_0 and kB^{-1}, which results in biases at some z/z_0 and kB^{-1}conditions. Therefore, to avoid the iteration process and keep the accuracy at the same time, this paper proposes a group of equations that divide the calculation into 8 regions according to z_0 and z_{0h} values. Section 2 describes the calculation results from CB05 and WRL12. Section 3 introduces the new equations, and Sect. 4 intercompares these schemes. Summary and conclusions are presented in Sect. 5

GMDD
6, 6459–6492, 2013

2 Revisiting CB05 and WRL12

The momentum flux τ and sensible heat flux H are defined as:

$$\tau \equiv \rho u_*^2 \tag{1}$$

$$H \equiv -\rho c_p u_* \theta_* \tag{2}$$

Here u_* is the friction velocity, θ_* is the temperature scale, ρ the air density and c_p the specific heat capacity at constant pressure. Based on MOST, the friction velocity u_* and temperature scale θ_* can be calculated by:

$$u_* = uk/\left[\ln\left(\frac{z}{z_0}\right) - \psi_{\mathrm{m}}\left(\frac{z}{L}\right) + \psi_{\mathrm{m}}\left(\frac{z_0}{L}\right) + \psi_{\mathrm{m}}^*\left(\frac{z}{L},\frac{z}{z_*}\right)\right] \tag{3}$$

$$\theta_* = (\theta - \theta_0)k/\left[\ln\left(\frac{z}{z_{0h}}\right) - \psi_{\mathrm{h}}\left(\frac{z}{L}\right) + \psi_{\mathrm{h}}\left(\frac{z_{0\mathrm{h}}}{L}\right) + \psi_{\mathrm{h}}^*\left(\frac{z}{L},\frac{z}{z_*}\right)\right] \tag{4}$$

Here u and θ are the wind speed and potential temperature at the reference height z. k is the von Karman constant. z_* is the roughness sublayer height. θ_0 is the potential temperature at the height of z_{0h}. ψ_{m} and ψ_{h} are the integrated stability functions for momentum and heat, respectively. ψ_{m}^* and ψ_{h}^* are the correction functions account for roughness sublayer effect. L is the Obukhov length defined as:

$$L \equiv u_*^2\overline{\theta}/(kg\theta_*) \tag{5}$$

ψ_{m}^* and ψ_{h}^* are given by De Ridder (2010):

$$\psi_{\mathrm{m,h}}^*\left(\frac{z}{L},\frac{z}{z_*}\right) = \int_z^{\infty} \frac{\phi_{\mathrm{m,h}}\left(\frac{z'}{L}\right)}{z'} e^{-\mu_{\mathrm{m,h}}\frac{z'}{z_*}} dz' \tag{6}$$

$\mu_{\mathrm{m}} = 2.59$, $\mu_{\mathrm{h}} = 0.95$, and $\phi_{\mathrm{m,h}}$ are the stability functions for momentum and heat. Following Sarkar and De Ridder (2010) and WRL12, $z_*/z_0 = 16.7$ is adopted in this study.

GMDD
6, 6459–6492, 2013
An improved surface flux scheme
Y. Li et al.

CB05 gives the form of $\phi_{\mathrm{m,h}}$ and $\psi_{\mathrm{m,h}}$:

$$\phi_{\mathrm{m}} = 1 + a\frac{\zeta + \zeta^{b}(1+\zeta^{b})^{\frac{1-b}{b}}}{\zeta + (1+\zeta^{b})^{\frac{1}{b}}} \tag{7}$$

$$\phi_{\mathrm{h}} = 1 + c\frac{\zeta + \zeta^{d}(1+\zeta^{d})^{\frac{1-d}{d}}}{\zeta + (1+\zeta^{d})^{\frac{1}{d}}} \tag{8}$$

$$\psi_{\mathrm{m}} = -a\ln(\zeta + (1+\zeta^{b})^{\frac{1}{b}}) \tag{9}$$

$$\psi_{\mathrm{h}} = -c\ln(\zeta + (1+\zeta^{d})^{\frac{1}{d}}) \tag{10}$$

Here $a = 6.1$, $b = 2.5$, $c = 5.3$ and $d = 1.1$. $\zeta = z/L$ is the stability parameter.

With Eqs. (3)–(6), $\phi_{\mathrm{m,h}}$ and $\psi_{\mathrm{m,h}}$ of CB05, fluxes can be calculated through iterations: with a first guess of ζ, u_* and θ_* can be calculated from Eqs. (3) and (4), then ζ again can be derived from Eq. (5). This procedure iterates until the results converge. The relationships of $\zeta \sim Ri_{\mathrm{B}}$, $\zeta \sim \ln(z/z_0)$, and $\zeta \sim \ln(z_0/z_{0h})$ from CB05 are shown in Figs. 1, 2 and 3, respectively. However, due to the limitation of computational time in numerical weather and climate models, the calculation results after 5 steps are always taken to approximate the fluxes (e.g., MYJ and MYNN surface module in WRF model, Janjić, 1996, Nakanishi M, Niino, 2006). It is found that with the first guess of $\zeta_0 = Ri_{\mathrm{B}}\frac{[\ln(z/z_0)]^2}{\ln(z/z_{0h})}$ and 5 steps of iteration, the results are still far away from the precise value. The relative error $\Delta\zeta$ that is calculated by Eq. (11) can exceed 70 % under certain conditions (Fig. 4).

$$\Delta\zeta = \begin{cases} \frac{\left|\zeta_{(\mathrm{cal})} - \zeta_{(\mathrm{precise})}\right|}{\zeta_{(\mathrm{precise})}} \times 100\%, \text{for} \left|\zeta_{(\mathrm{cal})} - \zeta_{(\mathrm{precise})}\right| \geq 0.01 \\ 0, \text{for} \left|\zeta_{(\mathrm{cal})} - \zeta_{(\mathrm{precise})}\right| < 0.01 \end{cases} \tag{11}$$

where $\zeta_{(\mathrm{cal})}$ is the calculation result, and $\zeta_{(\mathrm{precise})}$ is the precise result from the ultimate iteration of CB05 (when $|\zeta_{(n+1)} - \zeta_{(n)}| < 0.1\,\%\zeta_{(n)}$, $\zeta_{(n)}$ is adopted as $\zeta_{(\mathrm{precise})}$, and here

GMDD
6, 6459–6492, 2013
An improved surface flux scheme
Y. Li et al.

n indicates the iteration step). Under some other conditions, more than 80 steps of iteration are needed to reduce the calculation error within 5 % (Fig. 5). The iteration takes more steps to converge when there is a larger aerodynamic roughness length z_0 and a smaller thermal roughness length z_{0h}, which is common over an urban surface (Sugawara and Narita, 2009). When $z/z_0 = 10$ and $kB^{-1} = 30$, the largest error can reach 75 % after 5 steps iteration (Fig. 4) and 82 steps are needed for the results to converge (Fig. 5). However, when z/z_0 becomes large, for example $z/z_0 = 10^5$ (i.e., a representative value for a smooth sea surface), 5 steps are enough for the results to be within 5 % error under all kB^{-1} and Ri_B conditions (Fig. 5).

To avoid the iteration, and based on CB05's iteration results, WRL12 proposed the following set of equations:

$$\zeta_t = -0.316 - 0.515 e^{-L_{0\mathrm{H}}} + 25.8 e^{-2L_{0\mathrm{H}}} + 4.36 L_{0\mathrm{H}}^{-1} - 6.39 L_{0\mathrm{H}}^{-2} + 0.834 \log(L_{0\mathrm{M}}) - 0.0267 \log^2(L_{0\mathrm{M}}), \tag{12}$$

$$Ri_{\mathrm{B},t} = \zeta_t \frac{L_{0\mathrm{H}}^* + S_{0\mathrm{H}}^* \beta_\mathrm{H} \zeta_t}{(L_{0\mathrm{M}}^* + S_{0\mathrm{M}}^* \beta_\mathrm{M} \zeta_t)^2}, \tag{13}$$

$$\zeta = \frac{-L_{0\mathrm{M}}^*}{S_{0\mathrm{M}}^* \beta_\mathrm{M}} - \frac{BC}{4(S_{0\mathrm{M}}^* \beta_\mathrm{M})^3 (B^2 + |Cr|)} + \frac{B - \sqrt{B^2 + Cr} + \frac{BCr}{2(B^2 + |Cr|)}}{2(S_{0\mathrm{M}}^* \beta_\mathrm{M})^3 r}, (\text{for } Ri_\mathrm{B} < Ri_{\mathrm{B},t}), \tag{14}$$

$$\zeta = \zeta_t + D(\zeta_t)(Ri_\mathrm{B} - Ri_{\mathrm{B},t}), (\text{for } Ri_\mathrm{B} \geq Ri_{\mathrm{B},t}), \tag{15}$$

$$D(\zeta_t) = \frac{(L_{0\mathrm{M}}^* + S_{0\mathrm{M}}^* \beta_\mathrm{M} \zeta_t)^3}{L_{0\mathrm{M}}^* L_{0\mathrm{H}}^* + \zeta_t (2 S_{0\mathrm{H}}^* \beta_\mathrm{H} L_{0\mathrm{M}}^* - S_{0\mathrm{M}}^* \beta_\mathrm{M} L_{0\mathrm{H}}^*)}, \tag{16}$$

where

$$L_{0i} = \ln(z/z_{0i}), \quad (i \text{ stands for M or H}), \tag{17}$$

$$L_{0i}^{*} = L_{0i} + \frac{1}{\lambda}\ln\left(1+\frac{\lambda}{\mu_i \frac{z}{z_*}}\right) e^{-\mu_i \frac{z}{z_*}}, (i \text{ stands for M or H}), \tag{18}$$

$$r = Ri_{\mathrm{B}} - S_{0\mathrm{H}}^{*}\beta_{\mathrm{H}}/(S_{0\mathrm{M}}^{*}\beta_{\mathrm{M}})^2 \tag{19}$$

$$B = S_{0\mathrm{M}}^{*}\beta_{\mathrm{M}}L_{0\mathrm{M}}^{*} - 2S_{0\mathrm{H}}^{*}\beta_{\mathrm{H}}L_{0\mathrm{H}}^{*} \tag{20}$$

$$C = 4(S_{0\mathrm{M}}^{*}\beta_{\mathrm{M}})^2 L_{0\mathrm{M}}^{*}(S_{0\mathrm{H}}^{*}\beta_{\mathrm{H}}L_{0\mathrm{M}}^{*} - S_{0\mathrm{M}}^{*}\beta_{\mathrm{M}}L_{0\mathrm{H}}^{*}) \tag{21}$$

$$S_{0i}^{*} = 1 - z_{0i}/z + \left(1+\frac{\nu}{\mu_i \frac{z}{z_*}}\right)\frac{1}{\lambda}\ln\left(1+\frac{\lambda}{\mu_i \frac{z}{z_*}}\right) e^{-\mu_i \frac{z}{z_*}} \tag{22}$$

where $\lambda = 1.5$, $\nu = 0.5$, $\beta_{\mathrm{M}} = 4.76 + 7.03z_0/z + 0.24z_{0h}/z_0$ and $\beta_{\mathrm{H}} = 5$. First, $Ri_{\mathrm{B},t}$ is calculated from Eqs. (12) and (13), and then ζ can be derived from Eqs. (14) or (15). However, compared to the iterated results of CB05, the relative error of WRL12 exceeds 20 % when Ri_{B} is small, and exceeds 50 % when Ri_{B} becomes large (Fig. 6).

3 Derivation of the new scheme

It can be seen from Figs. 1–3 that ζ varies with Ri_{B}, $\log(z/z_0)$ and kB^{-1} with remarkable nonlinearity. Specially, when kB^{-1} is large, $\zeta \sim z_0$relationship can hardly be approximated by a cubic equation at some Ri_{B} values (Fig. 2). Correspondingly, when z_0 is large, $\zeta \sim z_{0h}$ also needs a high power series equation to approximate (at least cubic fit is not enough, Fig. 3). Therefore, similar to the division of Ri_{B} into weakly and strongly stable conditions in order to reduce the complexity of regression (e.g., Lauriainen, 1991; Li et al., 2010; WRL12), in this paper, multiple regions are divided with z_0 and z_{0h} values and regressions of $\zeta = f\left(Ri_{\mathrm{B}}, L_{0\mathrm{M}}, kB^{-1}\right)$ are conducted in these regions. In this way, the complexity of the equations can be reduced and at the same time their accuracy can be maintained. Although the total number of equations is increased due to the division of z_0 and z_{0h}, the calculation efficiency is still enhanced since the logical judgment of the region according to z_0 and z_{0h} values in programme codes takes much less time than iterations. The critical issue here is how to divide the z_0 and z_{0h} regions in a reasonable way to obtain the smallest number of regions but the highest accuracy. For this purpose, the z_0 and z_{0h} are first divided into 13 and 14 sections according to the values of z/z_0 and z_0/z_{0h}, respectively. For z/z_0, the sections are 10–20, 20–40, 40–80, ..., 10 240–20 480, 20 480–40 960 and 40 960–10^5; for z_0/z_{0h}, the sections are 0.607–1, 1–10, 10–100, 100–10^3, 10^3–10^4, ..., 10^{11}–10^{12} and 10^{12}–1.07×10^{13}. $z/z_0 \in 10 \sim 20$ and $z_0/z_{0h} \in 10^{12} \sim 1.07\times10^{13}$ is the region that needs the highest power series equation to approximate. This region is firstly chosen to find a maximum critical value of ζ_{c1} that can make the regression:

$$\zeta = f\left(Ri_\mathrm{B}, L_{0\mathrm{M}}, kB^{-1}\right) = Ri_\mathrm{B}\sum C_{ijk} Ri_\mathrm{B}^{i} L_{0\mathrm{M}}^{j} (L_{0\mathrm{H}} - L_{0\mathrm{M}})^k \tag{23}$$

be within 5 % error when $\zeta \in 0 \sim \zeta_{c1}$. Here i, j, and $k = 0, 1, 2$, and 3, and $i + j + k \le 4$. C_{ijk} are the coefficients from regression. It is found that $\zeta_{c1} = 0.33$ meets this criterion. Then some of the z_0 and z_{0h} regions can be merged with each other for the section $\zeta \in 0 \sim 0.33$ and a total of 8 $z_0 - z_{0h}$ regions are left in the $z_0 - z_{0h}$ plane. In other words, the regression error of Eq. (23) can be kept within 5 % in any of the 8 regions when $\zeta \in 0 \sim 0.33$ (Table 1). Thus, for these 8 regions, it can be found that with the sections divided by the specified critical values ζ_{cp} (where p is $1, 2, 3, \ldots$ it indicates the section and its maximum value depends on the $z_0 - z_{0h}$ region), the regression error with Eq. (23) can be kept within 5 % for $\zeta \le 0.5$ and 10 % or $\zeta > 0.5$. For a given pair of z_0 and z_{0h}, the division by ζ_{cp} can be transformed to $Ri_{\mathrm{B}cp}$:

$$Ri_{\mathrm{B}cp} = \sum C_{mn} \log^m(L_{0\mathrm{M}})(L_{0\mathrm{H}} - L_{0\mathrm{M}})^n \tag{24}$$

Here m, $n = 0$, 1, 2, and $m + n \le 3$; p is $1, 2, 3, \ldots$, which indicates the section and its maximum value depends on the $z_0 - z_{0h}$ region. For region 1 and 7, the maximum p

GMDD
6, 6459–6492, 2013

is 6, while for other regions it varies between 3 and 5. The coefficients for Eq. (24) are shown in Table 2. The Ri_{Bcp} then cut the 0–2.5 Ri_B range into several sections: Sect. 1 is from 0 to Ri_{Bc1}, Sect. 2 from Ri_{Bc1} to Ri_{Bc2}, and so on. The coefficients for Eq. (23) in each section are given in Tables 3–10. The calculation procedure for a given group of z_0, z_{0h} and Ri_B is that: (1) find the region according to z_0 and z_{0h} with Table 1; (2) Find the section according to the region and Ri_B with Eq. (24) and coefficients in Table 2; and (3) In Table 3–10 find the coefficients for the particular region and section and use Eq. (23) to calculate ζ. With the new equations, the relative error is controlled to be within 10 % for the whole range (Fig. 7). Specially, when $\zeta \leq 0.5$, the relative error is within 5 % since it happens more often in the real conditions (Fig. 8).

4 Comparison of the results from CB05 with 5 steps iteration, WRL12 and the new scheme

The maximum and average relative error of ζ, C_M and C_H calculated from CB05 with 5 steps iteration, WRL12 and the new scheme are shown in Figs. 8–10. C_M and C_H are the transfer coefficients for momentum and sensible heat respectively, and:

$$C_M = \frac{k^2}{\left[\ln\left(\frac{z}{z_0}\right) - \psi_m(\zeta) + \psi_m\left(\frac{z_0}{z}\zeta\right) + \psi_m^*\left(\zeta, \frac{z}{z_*}\right)\right]^2} \tag{25}$$

$$C_H = \frac{k^2}{\left[\ln\left(\frac{z}{z_0}\right) - \psi_m(\zeta) + \psi_m\left(\frac{z_0}{z}\zeta\right) + \psi_m^*\left(\zeta, \frac{z}{z_*}\right)\right]\left[\ln\left(\frac{z}{z_{0h}}\right) - \psi_h(\zeta) + \psi_h\left(\frac{z_0}{z}\zeta\right) + \psi_h^*\left(\zeta, \frac{z}{z_*}\right)\right]} \tag{26}$$

To speed up the calculation, $\psi^*_{\mathrm{m,h}}(\zeta, \frac{z}{z_*})$ here is not calculated from Eq. (6) but rather from the non-integral equation proposed by De Ridder (2010):

$$\psi^*_{\mathrm{m,h}}\left(\zeta, \frac{z}{z_*}\right) = \phi_{\mathrm{m,h}}\left[\left(1 + \frac{\nu}{\mu z/z_*}\right)\zeta\right]\frac{1}{\lambda}\ln\left(1 + \frac{\lambda}{\mu z/z_*}\right)\exp(\mu z/z_*) \quad (27)$$

Where $\lambda = 1.5$, $\mu = \mu_\mathrm{m} = 2.59$, $\mu = \mu_\mathrm{h} = 0.95$ and $\nu = 0.5$. The relative error for C_M and C_H is calculated from:

$$\Delta C_{\mathrm{M,\,H}} = \frac{\left|C_{\mathrm{M,\,H(cal)}} - C_{\mathrm{M,\,H(precise)}}\right|}{C_{\mathrm{M,\,H(precise)}}} \times 100\% \quad (28)$$

where $C_{\mathrm{M,\,H(cal)}}$ is calculated with $\zeta_{\mathrm{(cal)}}$ from the three different methods, and $C_{\mathrm{M,\,H(precise)}}$ is calculated with $\zeta_{\mathrm{(precise)}}$ from the ultimate iteration of CB05.

Maximum error indicates the maximum error for a particular ζ under various z_0 and z_{0h} conditions, while average error is calculated from

$$\mathrm{AverageError}(\zeta) = \frac{\int_{-0.5}^{30}\int_{\log(10)}^{\log(10^5)} \mathrm{Error}(\zeta)\,\mathrm{d}\log\left(\frac{z}{z_0}\right)\mathrm{d}\log\left(\frac{z_0}{z_{0h}}\right)}{\int_{-0.5}^{30}\int_{\log(10)}^{\log(10^5)} \mathrm{d}\log\left(\frac{z}{z_0}\right)\mathrm{d}\log\left(\frac{z_0}{z_{0h}}\right)} \quad (29)$$

Here Error(ζ) indicates $\Delta\zeta$ or $\Delta C_{\mathrm{M,\,H}}$ at a particular ζ. Although Eq. (28) presents the form of continuous integral, it is actually calculated discretely with interval 0.035 for $\log(\frac{z}{z_0})$ and 0.1 for $\log(\frac{z_0}{z_{0h}})$.

The results indicate that the maximum $\Delta\zeta$can be significant (exceeds 50 %) when using CB05 with 5 steps iteration or WRL12. Correspondingly, the average $\Delta\zeta$ for the two methods both exceeds 15 %. While with the new scheme, the maximum $\Delta\zeta$ is always smaller than 5 % (when $\zeta \le 0.5$) and 10 % (when $\zeta > 0.5$), and the average $\Delta\zeta$

GMDD
6, 6459–6492, 2013

is always smaller than 2 % in the whole range. The maximum ΔC_{M} from CB05 with 5 steps iteration (WRL12) exceeds 50 % (40 %), and average ΔC_{M}exceeds 30 % (8 %). The maximum ΔC_{H} from CB05 with 5 steps iteration (WRL12) exceeds 50 % (24 %), and average ΔC_{H}exceeds 18 % (6 %). Comparatively, the new scheme controls the maximum $\Delta C_{\mathrm{M}}(\Delta C_{\mathrm{H}})$ to be within 12 % (9 %) and the average $\Delta C_{\mathrm{M}}(\Delta C_{\mathrm{H}})$ within 1 % (1 %).

5 Summary and conclusions

Although CB05 provides a way to calculate surface fluxes under stable condition, its practical usage is confined due to the involved iteration process. It has been shown that iteration with 5 steps will result in large calculation errors, especially when z/z_0 is small and kB^{-1} is large, which is common over an urban surface. WRL12 proposed a way to avoid the iteration, but its calculation accuracy can be improved. Through dividing the $z_0 - z_{0h}$ plane into 8 regions, the new scheme develops a group of equations with higher accuracy. The calculation error of $\zeta = f\left(Ri_{\mathrm{B}}, L_{0\mathrm{M}}, kB^{-1}\right)$ is always controlled to be within 5 % (when $\zeta \le 0.5$) and 10 % (when $\zeta > 0.5$). The calculation procedure is also simple, for a small Ri_{B} (i.e., $Ri_{\mathrm{B}} < Ri_{\mathrm{B}c1}$), only one time computation of Eqs. (23) and (24) will suffice. The maximum computation step is 6 times of Eq. (24) and one time of Eq. (23) when it is in region 1 or 7 and at the same time Ri_{B} is large (i.e., $Ri_{\mathrm{B}} > Ri_{\mathrm{B}c6}$). Note that the Eq. (24) has only a maximum of 8 elements and a minimum of 4 elements so the calculation is still efficient. Overall, the new equations cover the full range of $-0.5 \le kB^{-1} \le 30$, $10 \le z/z_0 \le 10^5$ and stable condition (i.e., $0 < Ri_{\mathrm{B}} \le 2.5$), and maintain high accuracy and efficiency. It is expected that its usage in climate and weather forecast models can lead to better performance in surface flux calculation under stable conditions, especially over urban surfaces.

Supplementary material related to this article is available online at http://www.geosci-model-dev-discuss.net/6/6459/2013/ gmdd-6-6459-2013-supplement.zip.

Acknowledgements. The authors would like to acknowledge P. A. Jiménez, J. Dudhia, J. F. González-Rouco, J. Navarro, J. P. Montávez, E. García-Bustamante, H. Wouters, K. De Ridder and N. P. M. van Lipzig. Their two recent papers make us aware of the deficiency of current surface layer flux schemes. This study is supported by the National Program on Key Basic Research Project of China (973) under grant 2010CB428502, China Meteorological Administration under grant GYHY201006024, National Natural Science Foundation of China under grant 41275022, the CAS Strategic Priority Research Program grant XDA05110101.

References

Beljaars, A. C. M. and Holtslag, A. A. M.: Flux parameterization over land surfaces for atmospheric models, J. Appl. Meteorol., 30, 327–341, 1991.

Businger, J. A.: Transfer of momentum and heat in the planetary boundary layer, in: Proceedings of the symposium on the Arctic heat budget and atmospheric circulation, 305–331, 1966.

Businger, J. A., Wyngaard, J. C., Izumi, Y., and Bardley, E. F.: Flux-profile relationships in the atmospheric surface layer, J. Atmos. Sci., 28, 181–189, 1971.

Chen, F. and Dudhia, J.: Coupling an advanced land surface-hydrology model with the Penn State-NCAR MM5 modeling system, Part I: model implementation and sensitivity, Mon. Weather Rev., 129, 569–585, 2001.

Cheng, Y. G. and Brutsaert, W.: Flux-profile relationships for wind speed and temperature in the stable atmospheric boundary layer, Bound.-Lay. Meteorol., 114, 519–538, 2005.

De Bruin, H. A. R., Ronda, R. J., and Van De Wiel, B. J. H.: Approximate solutions for the Obukhov length and the surface fluxes in terms of bulk Richardson numbers, Bound.-Lay. Meteorol., 95, 145–157, 2000.

Dyer, A. J.: The turbulent transport of heat and water vapour in an unstable atmosphere, Q. J. Roy. Meteor. Soc., 93, 501–508, 1967.

Dyer, A. J.: A review of flux-profile relationships, Bound.-Lay. Meteorol., 7, 363–372, 1974.

Fairall, C. W., Bradley, E. F., Rogers, D. P., Edson, J. B., and Young, G. S.: Bulk parameterization of air-sea fluxes for TOGACOARE, J. Geophys. Res., 101, 3747–3764, 1996.
Garratt, J. R.: The Atmospheric Boundary Layer, Cambridge University Press, Cambridge, 1992.
Guo, X. and Zhang, H.: A performance comparison between nonlinear similarity functions in bulk parameterization for very stable conditions, Environ. Fluid Mech., 7, 239–257, 2007.
Högström, U.: Review of some basic characteristics of the atmospheric surface layer, Bound.-Lay. Meteorol., 78, 215–246, 1996.
Holtslag, A. A. M. and de Bruin, H. A. R.: Applied modelling of the nighttime surface energy balance over land, J. Appl. Meteorol., 22, 689–704, 1988.
Janjić, Z. I.: The step-mountain eta coordinate model: further developments of the convection, viscous sublayer and turbulence closure schemes, Mon. Weather Rev., 122, 927–945, 1994.
Janjić, Z. I.: The surface layer in the NCEP Eta Model. Eleventh conference on numerical weather prediction, Norfolk, VA, 19–23 August 1996, Amer. Meteor. Soc., Boston, MA, 354–355, 1996.
Jiménez, P. A., Dudhia, J., González-Rouco, J. F., Navarro, J., Montávez, J. P., and García-Bustamante, E.: A revised scheme for the WRF surface layer formulation, Mon. Weather Rev., 140, 898–918, 2012.
Launiainen, J.: Derivation of the relationship between the Obukhov stability parameter and the bulk Richardson number for flux-profile studies, Bound.-Lay. Meteorol. 76, 165–179, 1995.
Li, Y., Gao, Z., Lenschow, D. H., and Chen, F.: An improved approach for parameterizing surface-layer turbulent transfer coefficients in numerical models, Bound.-Lay. Meteorol., 137, 153–165, 2010.
Louis, J. F.: A parametric model of vertical eddy fluxes in the atmosphere, Bound.-Lay. Meteorol., 17, 187–202, 1979.
Monin, A. S. and Obukhov, A. M.: Dimensionless characteristics of turbulence in the surface layer of the atmosphere, Trudy. Geofiz. Inst. Akad. Nauk. SSSR, 24, 163–187, 1954.
Nakanishi, M. and Niino, H.: An improved Mellor–Yamada level-3 model: its numerical stability and application to a regional prediction of advection fog, Bound.-Lay. Meteorol., 119, 397–407, 2006.
Paulson, C. A.: The mathematical representation of wind speed and temperature in the unstable atmospheric surface layer, J. Appl. Meteor., 9, 857–861, 1970.

GMDD
6, 6459–6492, 2013
An improved surface flux scheme
Y. Li et al.

Sugawara, H. and Narita, K.: Roughness length for heat over an urban canopy, Theor. Appl. Climatol., 95, 291–299, 2009.
Skamarock, W. C., Klemp, J. B., Dudhia, J., Gill, D. O., Barker, D. M., Wang, W., and Powers, J. G.: A description of the advanced research WRF version 3, NCAR Technical Note, 2008.
Song, Y.: An improvement of the Louis scheme for the surface layer in an atmospheric modelling system, Bound.-Lay. Meteorol. 88, 239–254, 1998.
Wouters, H., De Ridder, K., and van Lipzig, N. P. M.: Comprehensive parametrization of surface-layer transfer coefficients for use in atmospheric numerical models, Bound.-Lay. Meteorol.: 145, 539–550, 2012.
Yang, K., Tamai, N., and Koike, T.: Analytical solution of surface layer similarity equations, J. Appl. Meteorol., 40, 1647–1653, 2001.

Table 1. The 8 regions divided by z/z_0 and z_0/z_{0h} values.

Region	z/z_0	z_0/z_{0h}
1	10–160	0.607–100
2	160–10^5	0.607–100
3	10–80	100–10^7
4	80–10^5	100–10^7
5	10–40	10^7–10^{11}
6	40–10^5	10^7–10^{11}
7	10–40	10^{11}–1.07×10^{13}
8	40–10^5	10^{11}–1.07×10^{13}

GMDD
6, 6459–6492, 2013

Table 2. The coefficients of Eq. (24).

Region		C_{00}	C_{10}	C_{20}	C_{01}	C_{11}	C_{21}	C_{02}	C_{12}
1	Ri_{Bc1}	0.3095	−0.2852	0.07955	0.03388	−0.01605	0	0	-1.079×10^{-4}
	Ri_{Bc2}	0.3219	−0.2613	0.06753	0.04838	−0.03101	0.003908	−0.00178	0.001165
	Ri_{Bc3}	0.3545	−0.2569	0.06609	0.05837	−0.03934	0.005643	−0.003381	0.002194
	Ri_{Bc4}	0.439	−0.3133	0.08619	0.0893	−0.07112	0.01403	−0.005965	0.003806
	Ri_{Bc5}	0.6887	−0.5375	0.1616	0.1754	−0.1564	0.03489	−0.01277	0.008101
	Ri_{Bc6}	1.706	−1.62	0.5231	0.5124	−0.5026	0.1239	−0.03577	0.02238
2	Ri_{Bc1}	0	0.08606	−0.03048	0.09019	−0.07682	0.01693	0	0
	Ri_{Bc2}	0.2002	0	−0.01589	0	0.00367	0	0.005057	−0.002399
	Ri_{Bc3}	0.4499	0	−0.02397	0.0388	−0.01145	0	0	0
3	Ri_{Bc1}	0.3063	−0.2849	0.07886	0.03104	−0.01423	-5.632×10^{-4}	3.684×10^{-6}	-2.926×10^{-6}
	Ri_{Bc2}	0.3555	−0.3002	0.07855	0.02617	−0.004769	−0.004012	-1.298×10^{-5}	9.907×10^{-6}
	Ri_{Bc3}	0.5064	−0.4282	0.1229	0.02138	0	−0.00441	0	0
	Ri_{Bc4}	1.638	−1.743	0.5813	0.04471	−0.01874	0	0	0
4	Ri_{Bc1}	0.09742	0	−0.01096	0.04544	−0.03299	0.006383	0	0
	Ri_{Bc2}	0.1768	0	−0.01434	0.03558	−0.02059	0.003327	0	0
	Ri_{Bc3}	0.3636	0	−0.0224	0.04607	−0.02506	0.004152	0	0
5	Ri_{Bc1}	0	0	0	0.04825	−0.01677	−0.004762	-5.212×10^{-4}	2.768×10^{-4}
	Ri_{Bc2}	0	0	0.08807	0.05219	−0.01822	−0.01245	-8.5×10^{-4}	7.516×10^{-4}
	Ri_{Bc3}	0	0	0.1219	0.0583	−0.02373	−0.01224	−0.001081	9.539×10^{-4}
	Ri_{Bc4}	0	0	0.1609	0.07789	−0.04617	−0.00736	−0.001399	0.001238
	Ri_{Bc5}	0.4437	0	0	0.1349	−0.1388	0.03347	−0.00119	0.001095
6	Ri_{Bc1}	0	0	0	0.05594	−0.03245	0.005037	-3.654×10^{-4}	1.135×10^{-4}
	Ri_{Bc2}	0.1945	0	0	0.03347	−0.02116	0.002301	0	8.92×10^{-5}
	Ri_{Bc3}	0.4288	−0.1436	0.01635	0.03207	−0.01382	0.001571	1.326×10^{-5}	-6.424×10^{-6}
7	Ri_{Bc1}	0	0	0	0.03681	−0.007664	−0.005619	-1.211×10^{-4}	0
	Ri_{Bc2}	0	0	0	0.03655	0	−0.009977	-2.691×10^{-4}	1.057×10^{-4}
	Ri_{Bc3}	0	0	0	0.03822	0	−0.01036	-3.658×10^{-4}	1.769×10^{-4}
	Ri_{Bc4}	0	0	0	0.0384	0	−0.009243	-3.629×10^{-4}	1.471×10^{-4}
	Ri_{Bc5}	0	0	0	0.05616	−0.02275	0	-5.172×10^{-4}	2.261×10^{-4}
	Ri_{Bc6}	0	0	0	0.1472	−0.1144	0.02796	−0.001218	5.835×10^{-4}
8	Ri_{Bc1}	0	0	0	0.05139	−0.02991	0.004664	-2.135×10^{-4}	6.535×10^{-5}
	Ri_{Bc2}	0	0	0	0.04919	−0.0197	0.002011	-3.325×10^{-4}	7.974×10^{-5}
	Ri_{Bc3}	0.5775	−0.2236	0.03477	0.03805	−0.01617	0.00177	-2.191×10^{-5}	1.067×10^{-5}

GMDD
6, 6459–6492, 2013

Table 3. The coefficients of Eq. (23) for Region 1.

	Region 1						
	Section 1	Section 2	Section 3	Section 4	Section 5	Section 6	Section 7
C_{00}	−1.134	0	0	0	0	0	0
C_{100}	31.1	86.35	−280.4	0	0	−17.32	−6.343
C_{200}	−71.16	0	3235	0	0	8.773	7.66
C_{300}	227.4	0	−6165	0	0	0	−0.7661
C_{001}	−0.2094	−11.53	−10.64	0	0	0	0.0125
C_{101}	3.293	194.9	193.8	0	1.113	0	−2.203
C_{201}	−20.11	−975.4	−1194	−12.37	−97.56	0	0.8896
C_{301}	14.42	1472	2161	0	159.4	0	−0.1273
C_{002}	0.1476	−2.535	−4.603	0	0	1.919	−0.00827
C_{102}	−0.07325	28.24	52.02	11.99	16.33	0	0.3327
C_{202}	0.5627	−61.13	−110.7	−15.63	−25.67	0.2679	−0.04613
C_{003}	−0.01178	−0.2378	−0.5367	−0.3157	−0.6447	−0.2892	0
C_{103}	0.0218	0.7405	1.503	0.2948	0.9718	0	−0.04968
C_{010}	1.405	13.6	30.26	0	6.821	10.27	7.513
C_{110}	−32.47	−316.2	−314.9	0	−57.13	0	0
C_{210}	46.59	1067	186	−108.1	227.3	0	−4.799
C_{310}	−38.25	−1494	0	317.8	−244	0	0.5598
C_{011}	−0.2286	8.023	9.038	0	0.9287	−3.457	−1.612
C_{111}	−1.097	−91.31	−87.06	−12.52	−17.88	−1.617	0
C_{211}	−0.3394	213.7	198.6	0	34.41	0	0
C_{012}	0	1.035	1.529	0	0.319	−0.07536	0.4666
C_{112}	0	−5.072	−7.439	−1.025	−2.452	0	0.0605
C_{013}	0	0.03622	0.07369	0.04669	0.08583	0.05146	−0.01808
C_{020}	0	−4.699	−10.71	−1.896	−2.195	−3.108	0
C_{120}	10.71	97.46	122.1	28.39	22.21	7.948	2.442
C_{220}	0	−152.4	−76.91	−14.19	−31.44	−2.985	0.1584
C_{021}	0	−1.704	−2.035	0	−0.1355	0.8751	0
C_{121}	0	9.069	8.248	2.214	1.976	0.3139	−0.04377
C_{022}	0	−0.09576	−0.1263	−0.01472	−0.04636	−0.05131	−0.0694
C_{030}	−0.00749	0.4446	1.015	0.3069	0.1708	0.2598	−0.1675
C_{130}	−0.9671	−7.991	−10.96	−3.635	−1.623	−0.8513	−0.2181
C_{031}	0.003402	0.1138	0.1426	−0.00877	0	−0.05427	0.05052

GMDD
6, 6459–6492, 2013

An improved surface flux scheme

Y. Li et al.

Table 4. Similar to Table 3, but for Region 2.

	Region 2			
	Section 1	Section 2	Section 3	Section 4
C_{00}	0	0	0	0
C_{100}	0	0	41.53	0
C_{200}	0	0	0	0
C_{300}	0	0	0	0
C_{001}	0	0	−1.616	−2.57
C_{101}	0	−12.35	0	−2.91
C_{201}	0	0	0	0
C_{301}	0	0	0	0
C_{002}	0	0	0	0.874
C_{102}	0	0.5183	0	0.3377
C_{202}	0	0	0	0
C_{003}	0	0	0	−0.00209
C_{103}	0	0	0	−0.01343
C_{010}	0.9996	0.8247	0	7.453
C_{110}	0	0	15.82	5.4
C_{210}	56.57	112.5	−27.37	−1.623
C_{310}	0	0	0	0.1999
C_{011}	−0.1456	−0.09054	0	0
C_{111}	0	0	0	0.4753
C_{211}	−12.1	−2.249	0	0
C_{012}	0	0.01653	0	−0.2047
C_{112}	0.1303	0	0.02288	−0.02581
C_{013}	0	0	0	0
C_{020}	0	0	0.1062	−0.9043
C_{120}	0.295	0.8326	−0.9992	−0.3386
C_{220}	0	−9.554	1.56	0.04556
C_{021}	0.005508	0	0	0.04682
C_{121}	−0.0359	0.07022	0	−0.01924
C_{022}	4.07×10^{-4}	−0.00133	0	0.01217
C_{030}	0	0	0	0.03944
C_{130}	0	0	0	0.006516
C_{031}	0	0	0	−0.00357

GMDD
6, 6459–6492, 2013

Table 5. Similar to Table 3, but for Region 3.

	Region 3				
	Section 1	Section 2	Section 3	Section 4	Section 5
C_{00}	2.001	0	−68.85	−1.514	0
C_{100}	−0.7876	0	756.9	0	0
C_{200}	0	0	−1100	0	0
C_{300}	60.42	368.9	0	19.63	0
C_{001}	−0.1401	3.514	0	0.559	0
C_{101}	−0.1085	−8.524	−30.13	0	0
C_{201}	−2.065	−18.05	86.99	0	0
C_{301}	−2.98	−4.852	5.71	−2.424	0
C_{002}	0.01334	0.08174	0.7274	−0.002248	0
C_{102}	0.0213	0.5791	−2.554	0	0
C_{202}	0.1963	0.1207	−0.2169	0.1259	0
C_{003}	-3.7×10^{-4}	−0.007021	0.01587	8.267×10^{-4}	2.413×10^{-4}
C_{103}	−0.002957	0	0.003912	−0.004141	7.107×10^{-5}
C_{010}	−1.442	1.207	76.25	−8.751	0
C_{110}	1.047	−31.68	−874.1	51.96	1.905
C_{210}	0	32.78	1636	−76.51	−1.761
C_{310}	0	−25.65	−1040	27.69	0.3658
C_{011}	0	−2.096	4.942	−1.349	−0.05227
C_{111}	0	2.222	−17.32	1.297	0
C_{211}	−1.121	0.3871	14.97	−0.09621	0
C_{012}	0	−0.004486	−0.09096	0	0
C_{112}	0.0273	−0.06669	0.2281	0	0
C_{013}	0	0.001086	−0.002971	2.192×10^{-4}	0
C_{020}	0.6868	−0.07632	−21.66	3.734	2.165
C_{120}	0	14.32	232.4	−6.438	0.6139
C_{220}	3.82	2.353	−224.1	6.284	−0.1166
C_{021}	−0.01898	0.3396	−1.724	0.2422	−0.07307
C_{121}	−0.1228	−0.3281	3.144	−0.2272	0.005656
C_{022}	2.845×10^{-4}	-3.6×10^{-4}	-4.477×10^{-4}	0	0
C_{030}	−0.06543	0	1.875	−0.4111	−0.3134
C_{130}	0.1469	−1.505	−18.02	0.2556	0
C_{031}	0.00179	−0.01529	0.1523	−0.009961	0.008105

GMDD
6, 6459–6492, 2013
An improved surface flux scheme
Y. Li et al.

Title Page
Abstract Introduction
Conclusions References
Tables Figures
◂◂ ▸▸
◂ ▸
Back Close
Full Screen / Esc
Printer-friendly Version
Interactive Discussion

Table 6. Similar to Table 3, but for Region 4.

	Region 4			
	Section 1	Section 2	Section 3	Section 4
C_{00}	0	−3.528	0	0
C_{100}	0	0	0	0
C_{200}	0	0	0	−8.306
C_{300}	0	0	0	1.212
C_{001}	0	−0.2511	−1.018	0
C_{101}	0	0	0	0
C_{201}	−6.267	−10.06	0	0
C_{301}	0	0	0	0
C_{002}	0	0	0	0
C_{102}	0.09808	0.1809	0	0.0279
C_{202}	0	0	0	0
C_{003}	0	0	6.735×10^{-5}	6.853×10^{-4}
C_{103}	0	0	0.001341	-9.314×10^{-4}
C_{010}	0.5961	1.375	−2.404	5.253
C_{110}	0	2.951	41.12	7.626
C_{210}	18.49	68.09	−48.05	−0.2889
C_{310}	34.53	0	24.94	0.06073
C_{011}	−0.0845	0	−0.06671	−0.3959
C_{111}	−0.5106	−1.361	0	−0.07098
C_{211}	−0.3543	0	−0.1319	0.003821
C_{012}	0.004555	0.003711	0.006818	0
C_{112}	0	0	0	0
C_{013}	-9.402×10^{-5}	0	-1.788×10^{-4}	0
C_{020}	0.05628	−0.02359	0.5172	−0.5006
C_{120}	0.8075	0.305	−4.023	−0.7376
C_{220}	0	−3.765	2.074	0
C_{021}	0	−0.001535	0	0.04853
C_{121}	0.01631	0.07098	0	0.002956
C_{022}	-3.8×10^{-5}	-2.577×10^{-4}	0	0
C_{030}	−0.00189	0	−0.0192	0.01968
C_{130}	−0.03755	0	0.125	0.025
C_{031}	5.177×10^{-5}	0	0	−0.001897

GMDD
6, 6459–6492, 2013

Table 7. Similar to Table 3, but for Region 5.

	Region 5					
	Section 1	Section 2	Section 3	Section 4	Section 5	Section 6
C_{00}	0	0	−207.7	−587.1	0	0
C_{100}	0	77.11	880	2726	7.886	0
C_{200}	−2.541	−201.2	−1550	−3759	−0.5889	0
C_{300}	25.22	386.1	2201	1605	0	0
C_{001}	−0.03201	−0.6831	0	−9.376	−0.4057	0
C_{101}	0.1159	0	11.61	−4.513	0	0
C_{201}	−0.5745	−7.571	−96.51	70.55	−0.5218	0
C_{301}	−0.8502	−8.978	0	−58.16	0	0
C_{002}	0.00208	0.07136	0.5093	0.1711	0.01745	0
C_{102}	−0.001668	0	0.8873	−0.9373	−0.01349	0
C_{202}	0.03737	0.3442	0.2868	1.132	0.01468	0
C_{003}	-1.828×10^{-5}	0	−0.01909	−0.006865	0	0
C_{103}	-3.967×10^{-5}	−0.003421	−0.004313	−0.001126	0	0
C_{010}	0.4298	0	189.4	286.9	0	0
C_{110}	−0.03339	−31.72	−543.8	−903.7	0	0
C_{210}	0.05692	2.558	324	407.6	0	0
C_{310}	0	0	−80.25	260.2	0	0.08919
C_{011}	−0.0233	0	−5.403	0	0	0
C_{111}	0	2.695	14.95	14.82	0.2908	0
C_{211}	−0.3158	−2.449	−1.706	−26.07	0.1992	0
C_{012}	0	−0.05044	−0.4221	0.01062	−0.003177	0
C_{112}	0.007595	0.05465	0.164	0.2099	−0.00933	0
C_{013}	0	-6.869×10^{-5}	−0.00111	9.863×10^{-4}	0	0
C_{020}	0	0.3612	−53.83	−44.24	0.7321	2.053
C_{120}	0	0	89.42	98.98	2.304	0.2534
C_{220}	1.793	18.63	34.6	22.67	−2.456	−0.2585
C_{021}	0.00249	0.1236	2.704	−0.01096	−0.09448	−0.0338
C_{121}	−0.05666	−0.837	−4.573	−1.67	0.007636	0.004269
C_{022}	0	0.008316	0.0718	−0.01056	0.002124	0
C_{030}	0	−0.06987	4.95	2.138	0	−0.3116
C_{130}	0.129	0.8756	−3.112	−4.604	0	0.1241
C_{031}	0	−0.01959	−0.3287	0.054	0	0

Table 8. Similar to Table 3, but for Region 6.

	Region 6			
	Section 1	Section 2	Section 3	Section 4
C_{00}	0	0.4383	0	−6.744
C_{100}	−7.864	0	−41.74	8.8
C_{200}	0	0	177	−13.03
C_{300}	0	0	−118.2	2.203
C_{001}	−0.02699	0	0	−0.1139
C_{101}	0.7414	−4.81	−4.006	−0.06103
C_{201}	−1.114	5.094	−0.5102	0.2406
C_{301}	0	−1.159	0	−0.04635
C_{002}	0	0.04547	0	0.01341
C_{102}	0	0	0.0567	−0.002749
C_{202}	0	−0.1233	0.1868	5.316×10^{-6}
C_{003}	0	-5.595×10^{-4}	0.002457	-1.434×10^{-4}
C_{103}	1.281×10^{-4}	0.002459	−0.006455	0
C_{010}	0.244	0	0	6.511
C_{110}	1.743	0	27.45	6.369
C_{210}	4.749	44.44	−17.37	−0.175
C_{310}	11.28	0	−7.74	0.03419
C_{011}	0	0	0	−0.3147
C_{111}	−0.3093	0	0	−0.06781
C_{211}	−0.2208	−0.6068	0.0117	-2.026×10^{-4}
C_{012}	0	−0.005459	−0.01576	0.002444
C_{112}	0.003674	0	0.02102	2.616×10^{-4}
C_{013}	0	0	-1.975×10^{-5}	-5.149×10^{-6}
C_{020}	0.04168	0	−0.1563	−0.6219
C_{120}	0.4341	0.9983	−2.085	−0.598
C_{220}	0.6518	−2.874	0.3443	0.002868
C_{021}	−0.00208	−0.00152	0.03278	0.03359
C_{121}	0	0.01501	−0.0325	0.003178
C_{022}	2.895×10^{-5}	3.541×10^{-4}	5.167×10^{-4}	-1.423×10^{-4}
C_{030}	0	0.006587	0.008163	0.02407
C_{130}	−0.01307	−0.04253	0.0854	0.0188
C_{031}	1.425×10^{-5}	-3.659×10^{-4}	−0.001602	−0.001167

GMDD
6, 6459–6492, 2013

An improved surface flux scheme

Y. Li et al.

Table 9. Similar to Table 3, but for Region 7.

	Region 7						
	Section 1	Section 2	Section 3	Section 4	Section 5	Section 6	Section 7
C_{00}	−1.412	−4.502	−104.2	542.4	178.4	0	0
C_{100}	6.658	40.44	136.3	−1845	158.8	0	0
C_{200}	−5.68	37.42	233.3	2157	−480.9	0	0
C_{300}	11.9	0	0	0	0	0	0
C_{001}	0.1285	0.3067	13.8	−3.691	−31.49	0	0
C_{101}	−0.111	−5.444	−37.21	3.33	47.56	0	0
C_{201}	−0.2095	2.053	10.33	−45.62	−4.153	0	0
C_{301}	−0.3181	0	0	0	0	0	0
C_{002}	−0.004693	0.05302	−0.1157	0.1434	0.3998	0	0
C_{102}	0.004467	0	0.5542	0.4557	−0.8692	0	0
C_{202}	0.01324	−0.01586	−0.2568	0.08936	0.2504	0	0
C_{003}	6.636×10^{-5}	0	0	0	0	0	0
C_{103}	-2.023×10^{-4}	0	0	0	0	0	0
C_{010}	0.7122	1.663	16.56	−263.7	−37.94	0	0
C_{110}	−4.599	−28.1	0	677.7	−147.8	20.56	0
C_{210}	2.705	−11.02	−114.4	−644.2	144.7	−13.42	0
C_{310}	0	0	0	0	0	3.002	0
C_{011}	−0.04962	0.1172	−3.238	4.44	9.904	−0.5254	0.06758
C_{111}	0.01147	1.979	7.578	−3.037	−7.914	0	0
C_{211}	−0.1621	−0.7285	0	10.93	−2.224	0	0.003671
C_{012}	0.001459	−0.0293	0	−0.08875	−0.1235	0	0
C_{112}	0.003514	0.01334	−0.06568	−0.1436	0.1631	0	-6.967×10^{-4}
C_{013}	-2.013×10^{-5}	0	0	0	0	2.282×10^{-4}	0
C_{020}	0.003692	−0.4475	0	32.93	0	0	0
C_{120}	1.299	5.193	−0.1495	−56.58	23.51	−2.349	0.6983
C_{220}	0.6516	5.593	18.12	53.14	−2.645	0.628	−0.1455
C_{021}	0	−0.009728	0.167	−0.951	−0.7278	0.2176	0
C_{121}	−0.03414	−0.3375	−0.6387	0	−0.1801	0.02067	0
C_{022}	2.835×10^{-5}	0.00347	0.00428	0.02119	0.008599	−0.005396	-4.282×10^{-4}
C_{030}	6.293×10^{-4}	0	0	0	0	−0.4148	0
C_{130}	−0.02559	0	0	0	0	0.02245	0
C_{031}	0	0	0	0	0	0.01163	0

Table 10. Similar to Table 3, but for Region 8.

	Region 8			
	Section 1	Section 2	Section 3	Section 4
C_{00}	−3.13	−49.55	0	0
C_{100}	5.26	97.14	0	0
C_{200}	−29.85	352.5	10.72	0
C_{300}	57.04	−573.4	0	0
C_{001}	0.2176	2.052	0	0
C_{101}	−0.00898	−21.41	0	0
C_{201}	−1.756	13.12	0	0
C_{301}	−1.663	20.82	−1.354	0
C_{002}	−0.007271	0.1357	−0.06227	0
C_{102}	0.0304	0.238	0	−0.01477
C_{202}	0.05349	−0.7316	0.08799	−0.001292
C_{003}	8.978×10^{-5}	−0.003367	0.002359	0
C_{103}	-6.252×10^{-4}	0.006023	−0.002387	3.921×10^{-4}
C_{010}	0.9846	14.57	−0.2492	0
C_{110}	−1.011	0	19.79	0
C_{210}	14.45	0	−18.86	−0.8522
C_{310}	4.433	−54.39	9.463	0.1065
C_{011}	−0.05083	−0.8911	0	0
C_{111}	−0.2604	1.478	0	0.374
C_{211}	−0.2977	2.13	−0.3291	0.004036
C_{012}	0.001361	-9.36×10^{-4}	0	0.002528
C_{112}	0.00375	−0.04272	0.01369	−0.006853
C_{013}	-1.464×10^{-5}	1.939×10^{-4}	-2.41×10^{-4}	-8.747×10^{-5}
C_{020}	−0.004659	−1.165	0	0
C_{120}	0.6393	0	−1.689	−0.4307
C_{220}	0	−3.616	1.036	0.01469
C_{021}	0	0.06747	0.00194	0.001642
C_{121}	0	0.01581	−0.02897	0
C_{022}	0	-3.126×10^{-4}	8.316×10^{-4}	0
C_{030}	8.014×10^{-4}	0.03485	0.01694	0
C_{130}	−0.01934	0	0.06734	0.01348
C_{031}	0	−0.001713	−0.001447	0

GMDD
6, 6459–6492, 2013
An improved surface flux scheme
Y. Li et al.

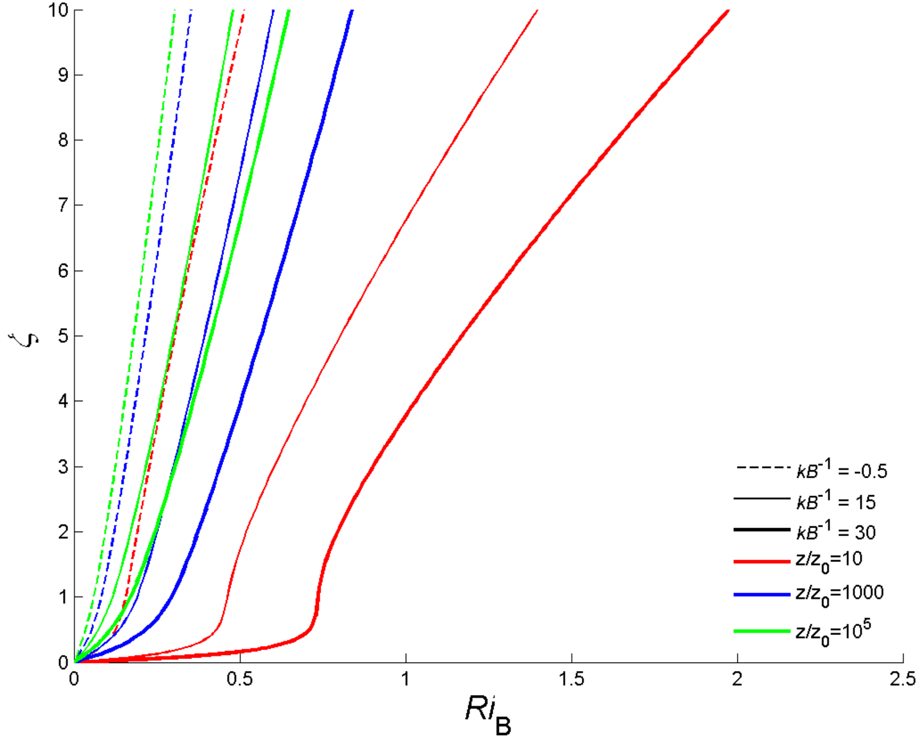

Fig. 1. The relationship between Ri_B and ζ from the precise results of CB05.

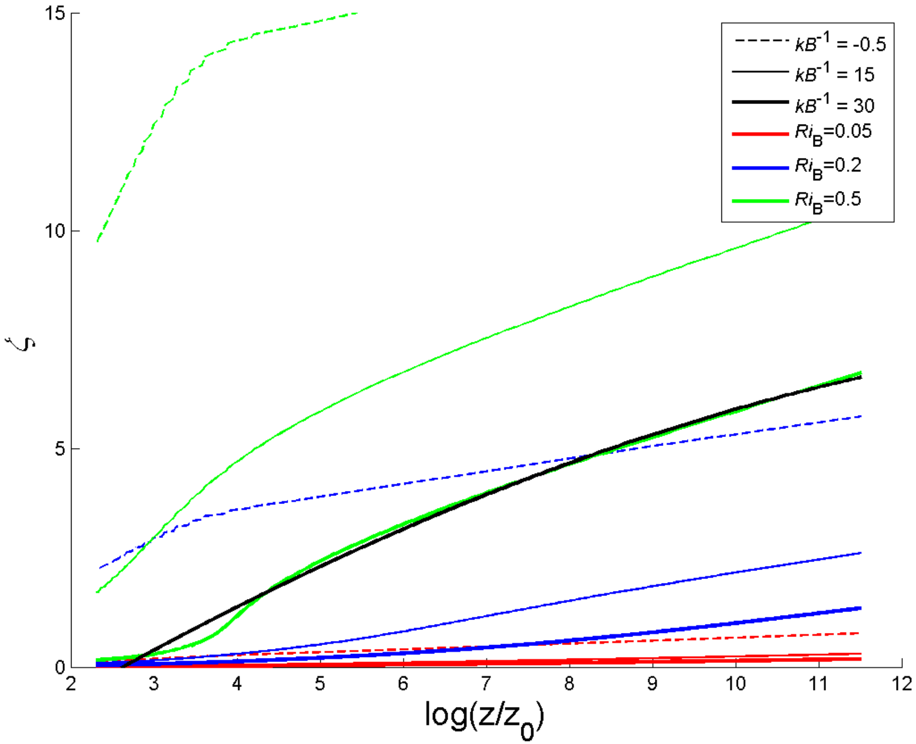

Fig. 2. The relationship between $\log(z/z_0)$ and ζ from the precise results of CB05. Black line indicates the cubic fit of curve $kB^{-1} = 30$ and $Ri_B = 0.5$with least square method.

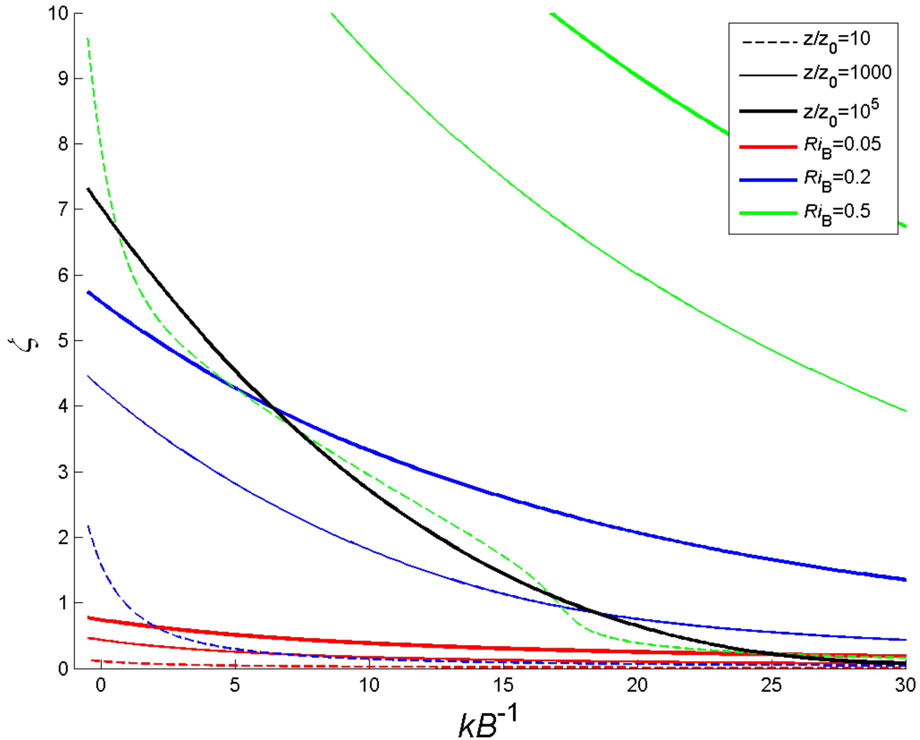

Fig. 3. The relationship between $\log(z/z_{0h})$ (i.e., kB^{-1}) and ζ from the precise results of CB05. Black line indicates the cubic fit of curve $z/z_0 = 10$ and $Ri_B = 0.5$ with least square method.

GMDD
6, 6459–6492, 2013

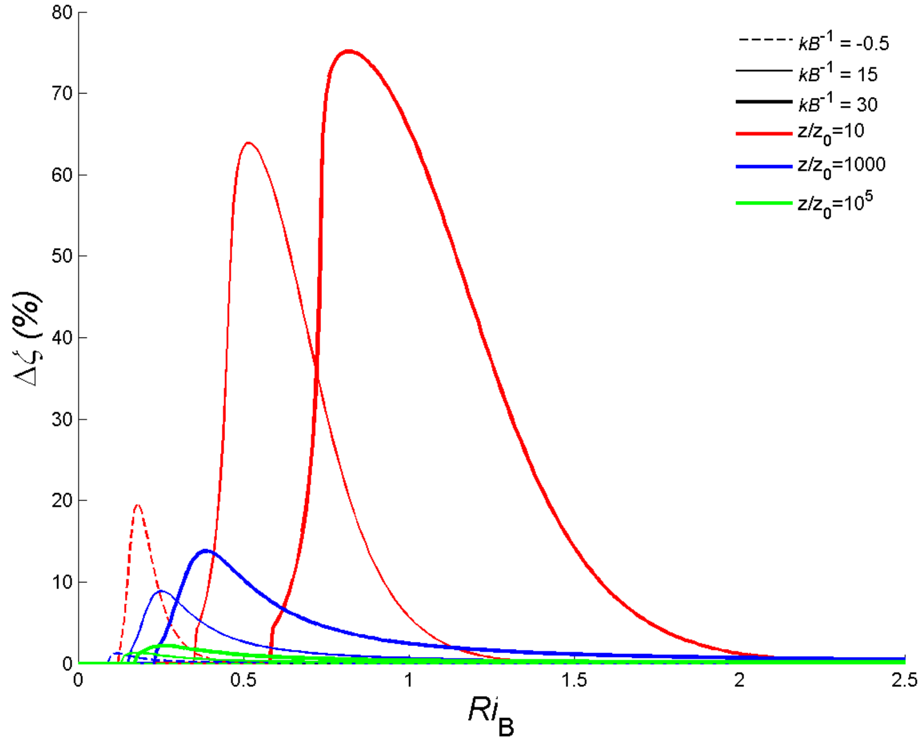

Fig. 4. Relative error after 5 steps of iteration with CB05 equations under certain z_0 and z_{0h} conditions.

GMDD
6, 6459–6492, 2013

An improved surface flux scheme

Y. Li et al.

Title Page
Abstract Introduction
Conclusions References
Tables Figures
Back Close
Full Screen / Esc
Printer-friendly Version
Interactive Discussion

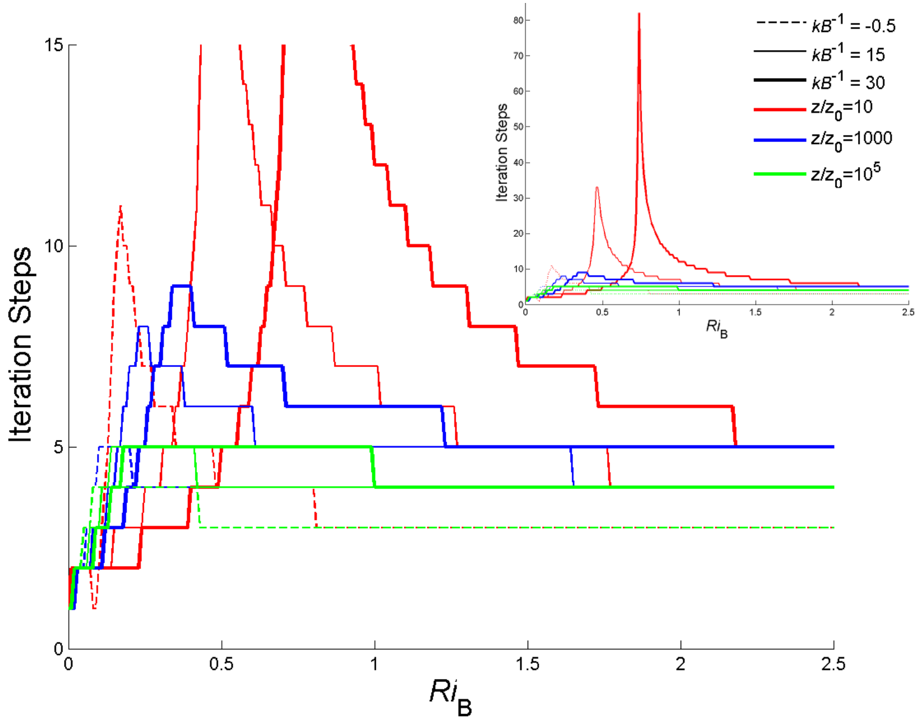

Fig. 5. Steps needed to converge into 5 % relative error with CB05 equations under certain z_0 and z_{0h} conditions. The inset shows the whole perspective.

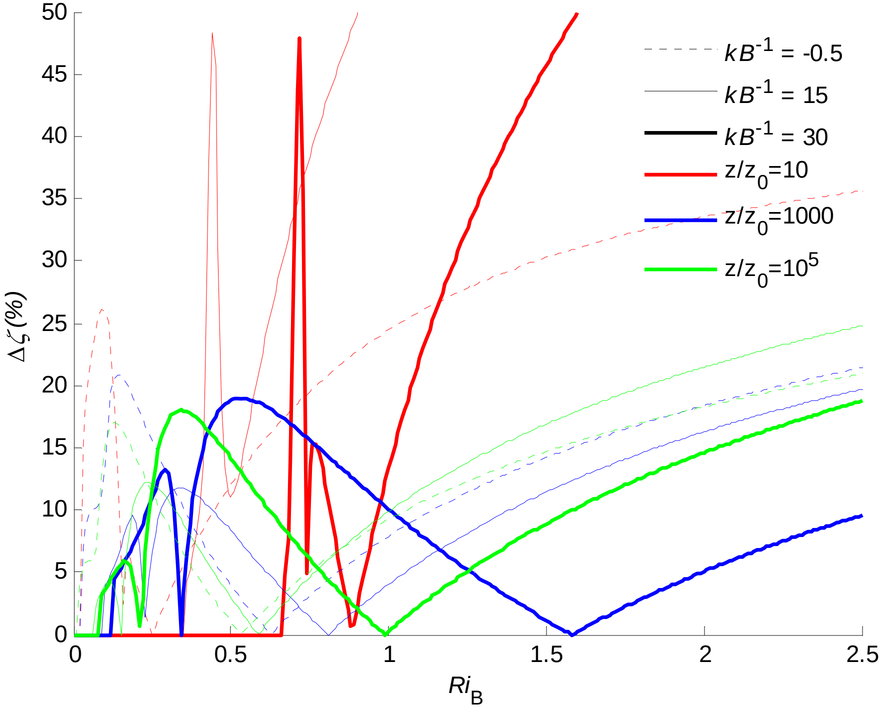

Fig. 6. Relative error with WRL12 equations.

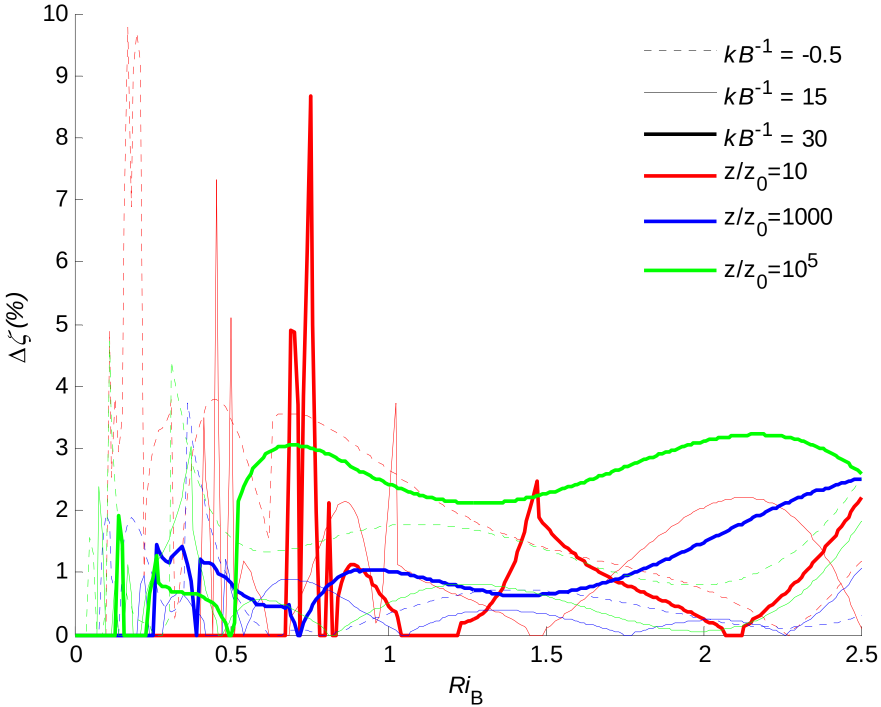

Fig. 7. Relative error with new equations.

GMDD
6, 6459–6492, 2013

An improved surface flux scheme

Y. Li et al.

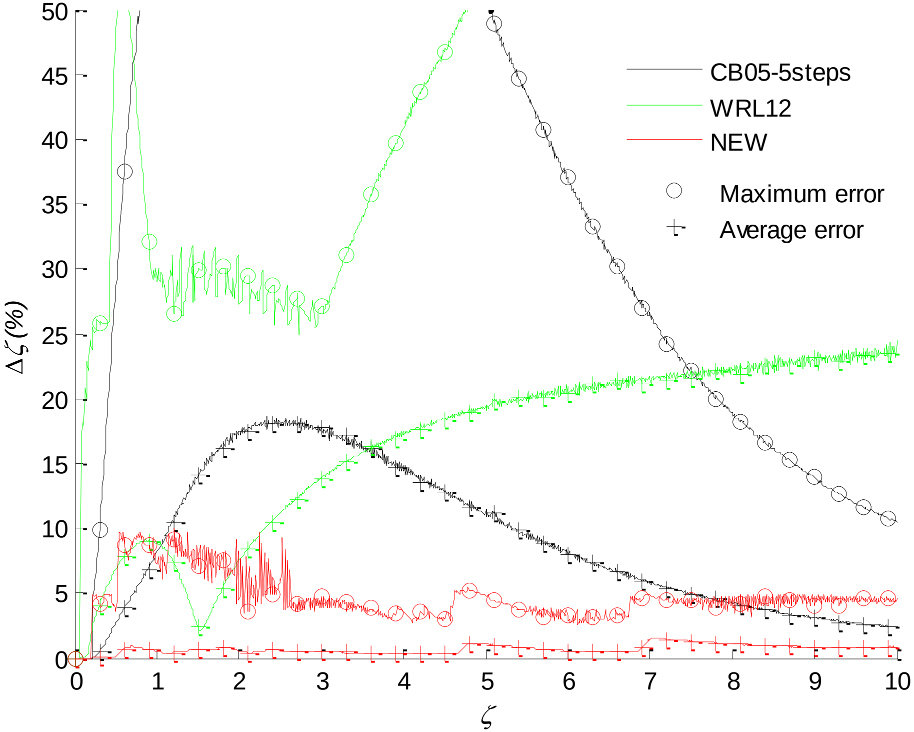

Fig. 8. Maximum (circles) and average (crosses) relative error of ζ for CB05 with 5 steps iteration (black lines), WRL12 (green lines) and the new scheme (red lines). Errors larger than 50 % are not shown.

GMDD
6, 6459–6492, 2013
An improved surface flux scheme
Y. Li et al.

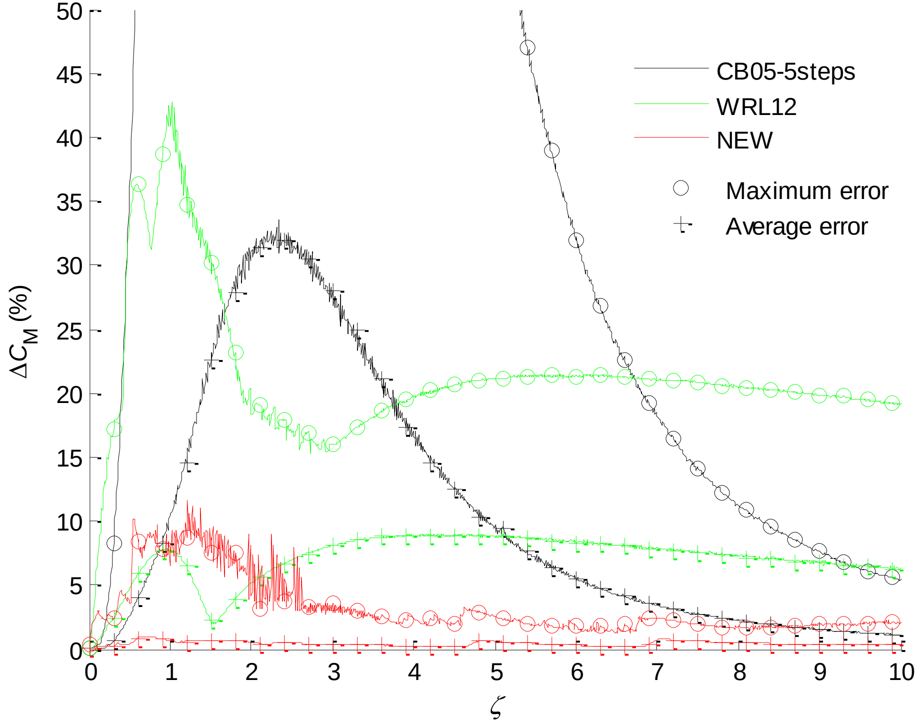

Fig. 9. Similar to Fig. 8 but for C_M.

GMDD
6, 6459–6492, 2013

An improved surface flux scheme

Y. Li et al.

Title Page
Abstract
Introduction
Conclusions
References
Tables
Figures
◀▎ ▶▎
◀ ▶
Back
Close
Full Screen / Esc
Printer-friendly Version
Interactive Discussion

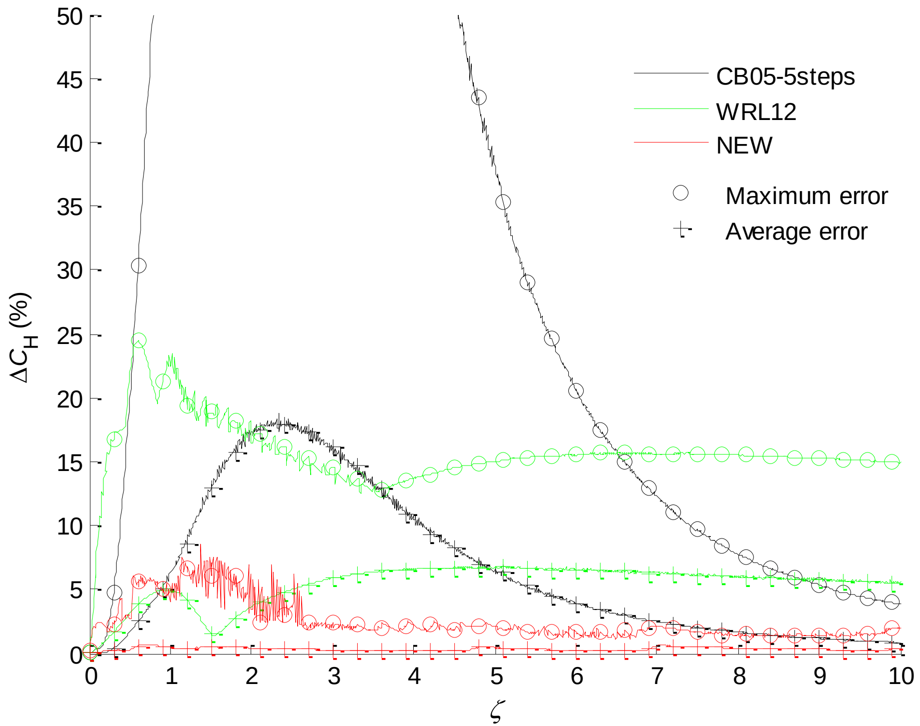

Fig. 10. Similar to Fig. 8 but for C_H.